lubricants

MDPI

Article

Influence of Al_2O_3 Nanoparticles Addition in ZA-27 Alloy-Based Nanocomposites and Soft Computing Prediction

Aleksandar Vencl [1,2,*], Petr Svoboda [3], Simon Klančnik [4], Adrian But [5], Miloš Vorkapić [6], Marta Harničárová [7,8] and Blaža Stojanović [9,*]

1 University of Belgrade, Faculty of Mechanical Engineering, Kraljice Marije 16, 11120 Belgrade, Serbia
2 South Ural State University, Lenin Prospekt 76, 454080 Chelyabinsk, Russia
3 Faculty of Mechanical Engineering, Brno University of Technology, Technická 2896/2, 616 69 Brno, Czech Republic
4 Faculty of Mechanical Engineering, University of Maribor, Smetanova 17, 2000 Maribor, Slovenia
5 Faculty of Mechanical Engineering, Politehnica University of Timișoara, Bulevardul Mihai Viteazu 1, 300222 Timișoara, Romania
6 University of Belgrade, Institute of Chemistry, Technology and Metallurgy, Njegoševa 12, 11000 Belgrade, Serbia
7 Institute of Electrical Engineering, Automation, Informatics and Physics, Faculty of Engineering, Slovak University of Agriculture, Tr. A. Hlinku 2, 949 76 Nitra, Slovakia
8 Faculty of Technology, Institute of Technology and Business in České Budějovice, Okružní 517/10, 370 01 České Budějovice, Czech Republic
9 University of Kragujevac, Faculty of Engineering, Sestre Janjić 6, 34000 Kragujevac, Serbia
* Correspondence: avencl@mas.bg.ac.rs (A.V.); blaza@kg.ac.rs (B.S.)

Abstract: Three different and very small amounts of alumina (0.2, 0.3 and 0.5 wt. %) in two sizes (approx. 25 and 100 nm) were used to enhance the wear characteristics of ZA-27 alloy-based nanocomposites. Production was realised through mechanical alloying in pre-processing and compocasting processes. Wear tests were under lubricated sliding conditions on a block-on-disc tribometer, at two sliding speeds (0.25 and 1 m/s), two normal loads (40 and 100 N) and a sliding distance of 1000 m. Experimental results were analysed by applying the response surface methodology (RSM) and a suitable mathematical model for the wear rate of tested nanocomposites was developed. Appropriate wear maps were constructed and the wear mechanism is discussed in this paper. The accuracy of the prediction was evaluated with the use of an artificial neural network (ANN). The architecture of the used ANN was 4-5-1 and the obtained overall regression coefficient was 0.98729. The comparison of the predicting methods showed that ANN is more efficient in predicting wear.

Keywords: ZA-27 alloy; Al_2O_3 nanoparticles; nanocomposites; wear; response surface methodology; artificial neural network

Citation: Vencl, A.; Svoboda, P.; Klančnik, S.; But, A.; Vorkapić, M.; Harničárová, M.; Stojanović, B. Influence of Al_2O_3 Nanoparticles Addition in ZA-27 Alloy-Based Nanocomposites and Soft Computing Prediction. *Lubricants* **2023**, *11*, 24. https://doi.org/10.3390/lubricants11010024

Received: 30 November 2022
Revised: 28 December 2022
Accepted: 30 December 2022
Published: 7 January 2023

1. Introduction

Metal matrix nanocomposites (MMnCs) can be defined as composites with metal base and one or several incorporated nano-sized secondary phases (mainly in particulate form). As in metal matrix composites, these secondary phase/phases usually have physical and mechanical properties very different from those of the matrix. Nowadays MMnCs can be produced by using various processing techniques [1], but the uniform distribution of the secondary phase/phases throughout the matrix is still a challenging task. The MMnCs can possess higher fracture strength and toughness, hardness and wear resistance over the matrix material. This is obtained through several strengthening mechanisms, i.e., load transfer effect, Hall–Petch strengthening, Orowan strengthening, coefficient of thermal expansion (CTE) and elastic modulus (EM) mismatch [2].

Regarding the matrix material, the majority of the researchers study aluminium- or magnesium-based nanocomposites, and significantly fewer researchers deal with zinc

alloy-based nanocomposites [3]. Among them, only a few investigated ZA-27 alloy-based nanocomposites with incorporated Al_2O_3 nanoparticles. Shivakumar et al. [4] investigated the ZA-27 alloy-base nanocomposites reinforced with 1, 3 and 5 wt. % Al_2O_3 nanoparticles (average size was 60–70 nm). Nanocomposites were obtained through stir casting accompanied by the squeeze casting technique. Wear tests were performed under the dry sliding conditions at four different normal loads (20, 40, 60 and 80 N) and four sliding speeds (1, 1.33, 1.67 and 2 m/s). The rotating counter-body was a hardened steel disc. Results showed that microhardness and wear resistance increase with the increase in the amount of nanoparticles.

Çelebi et al. [5] produced ZA-27 alloy-base nanocomposites with 1 wt. % Al_2O_3 nanoparticles (average size of 100 nm) through the hot pressing. Before the hot pressing, mechanical milling with variable time (from 1 to 8 h) was applied to mix the ZA-27 microparticles (average size of 40 μm) and Al_2O_3 nanoparticles. The results showed that an increase in milling time produced nanocomposites with higher porosity, but also higher macrohardness. On the other hand, the tensile strength of the nanocomposite initially increased and then rapidly decreased as the milling time increased. The main reason for these changes in the mechanical properties was the work hardening effect which makes the nanocomposites brittle. The work hardening was more pronounced for higher milling times.

Bobić et al. [6] also analysed the influence of milling time (from 30 to 180 min) during the pre-processing of the mixture used in the production of nanocomposites (compocasting process). Nanocomposites were with the ZA-27 alloy base and reinforced with 0.2, 0.3 and 0.5 wt. % Al_2O_3 nanoparticles of two different average sizes (25 and 100 nm). They found that the optimal time of 60 min provides improved macrohardness and compressive yield strength of the nanocomposites. They also noticed that all nanocomposites exhibited a finer structure of the matrix. The same nanocomposites, obtained with the optimal milling time, were also tested on erosion wear resistance with a solid particle impingement test (particles impact angle of 90°) [7]. The results showed that the presence of Al_2O_3 nanoparticles slightly increased erosive wear resistance due to the positive effect they have on the ductility of nanocomposites. Based on these positive results, the aim of this paper is to further study the ZA-27 alloy-based composites reinforced with 0.2, 0.3 and 0.5 wt. % Al_2O_3 nanoparticles of two different average sizes (25 and 100 nm). The novelty is that until now, there has been no tribological research on nanocomposites with such a low amount of nanoparticles and very few that covered ZA-27 alloy-based nanocomposites with incorporated alumina nanoparticles in higher amounts. Therefore, the effect of size and amount of added Al_2O_3 nanoparticles on microhardness and lubricated sliding wear resistance is investigated and analysed.

2. Experimental Details

2.1. Materials

The matrix material used to produce nanocomposites was zinc–aluminium alloy ZA-27, whose chemical composition is shown in Table 1. In total, six different nanocomposites were reinforced with Al_2O_3 particles. The amount of added Al_2O_3 particles varies (0.2, 0.3 and 0.5 wt. %), as well as their approximate sizes (25 and 100 nm). The equipment used for the manufacture of matrix alloy and nanocomposites is detailed elsewhere [8].

Table 1. Chemical composition (wt. %) of ZA-27 alloy.

Element	Al	Cu	Mg	Zn
Percentage	25–27	2.0–2.5	0.015–0.02	Balance

The matrix alloy was processed by the thixocasting (semi-solid processing). In order to remove the slag from the melt surface, the alloy was overheated to 550 °C. After that, the melt was cooled to 490 °C (at a rate of 5 °C/min) and its mixing at a rate of 500 rpm

began. With further cooling, the temperature reached 465 °C and at this temperature, the melt was mixed for 25 min. This intensive mixing resulted in the change in the structure of the primary particles of the matrix alloy, i.e., they become nondendritic. The melt was poured into the preheated (at 400 °C) steel mould, and after cooling at room temperature, the casts were additionally hot-pressed (at 370 °C and under 250 MPa).

The nanocomposites were produced by the compocasting process with mechanical alloying pre-processing (ball milling), which also started with preheating to 550 °C and cooling to 490 °C (with the introduction of mixing at 500 rpm). After that, the melt was cooled to 485 °C and the mixing rate was reduced to 250 rpm. At this point, the infiltration of the previously prepared (during ball milling) mixture of nanoparticles and metal chips [6,7] started and lasted for 4 min. During the infiltration the temperature was cooled to 465 °C, when the homogenisation of the composite melt started (still at 250 rpm) and lasted for 3 min. The mixing rate was then increased to 500 rpm and mixing continued for the next 20 min at a constant temperature. The nanocomposite melt was also poured into the preheated (at 400 °C) steel moulds, and after cooling at room temperature the casts were additionally hot-pressed (at 370 °C and under 250 MPa).

2.2. Methods of Characterisation

Plate-like samples (16 × 12 × 6 mm) were used for both microhardness and wear tests, i.e., microhardness was measured on the samples that were later used in wear testing. Measurements were according to the ASTM E384 standard. Vickers indenter and a load of 500 g (HV 0.5) with a dwell time of 15 s were used. At least five measurements were made for each sample in order to eliminate possible segregation effects and to obtain a representative value of the material microhardness.

Wear tests were carried out on a block-on-disc tribometer, according to the ASTM G77 standard, in lubricated sliding conditions with line contact between the block and disc of 6 mm. Blocks were made of tested materials, whereas the disc (counter-body) was made of quenched and tempered steel EN 42CrMo4 (51–54 HRC). The surface roughness of blocks and counter-body was approximately *Ra* = 0.14–0.17 μm and *Ra* = 0.6–0.7 μm, respectively. The lubricant was mineral gear oil (ISO VG 220, ISO L-CKC/CKD). Test parameters were: 0.25 and 1 m/s (sliding speeds), 1000 m (sliding distance) and 40 and 100 N (normal loads). The temperature of the oil was continually measured throughout each test. The average steady-state value of the temperature, i.e., the value at the end of the test was in the range of 30 ± 2 °C. The wear scar on the block was measured optically with an accuracy of 0.05 mm, after each test, in order to calculate the volume loss and compute the wear rate. Additionally, wear scars were utilised to determine the average pressure on contact surfaces at the end of the test, which in some cases reached 24 MPa. After testing, the worn surfaces of blocks were examined using the scanning electron microscope (SEM) equipped with an energy dispersive spectrometer (EDS). Samples were prepared through carbon evaporation where the thin carbon layer of 15–25 nm was deposited on samples.

2.3. Experimental Design

The used experimental design is presented in Table 2. The dependent variable was the wear rate of the tested nanocomposites, while the factors that affect this variable were Al_2O_3 amount, Al_2O_3 size, sliding speed and normal load. The first factor (Al_2O_3 amount) had four levels, and the other three factors (Al_2O_3 size, sliding speed and normal load) had two levels. Experimental results were analysed by applying the response surface methodology (RSM). The advantage of RSM is that it can provide quantitative measurements of possible interactions between influencing factors, which are difficult to obtain by other techniques [9]. The main idea of RSM is to use a sequence of designed experiments to obtain an optimal response [10,11]. It applies several mathematical and statistical techniques to develop an adequate functional dependence between the response (wear rate), and the influencing factors (Al_2O_3 amount, Al_2O_3 size, sliding speed and normal load).

Table 2. Influencing factors and their levels.

Factor	Unit	Level		
		1	2	3
A: Al_2O_3 amount	wt. %	0.2	0.3	0.5
B: Al_2O_3 size	nm	25	100	
C: sliding speed	m/s	0.25	1.00	
D: normal load	N	40	100	

The artificial neural network (ANN) simulation started with a "training" process in which a set of inputs are applied to the network. After that, the resulting set of outputs is compared to known values. The training is performed until the error between the output and known values reach a predefined value. ANN is usually used with a high amount of input data, but it can be used successfully for small data sets as well [12]. A feed-forward backpropagation multilayer ANN is employed, with three inputs, five neurons in the hidden layer and one output used (Figure 1). Networks with 2–25 neurons in the hidden layer were trained. Training and testing of the ANN are conducted using the software MATLAB R2016a. The logarithmic sigmoid transfer function (logsig) and linear transfer function (purelin) are used as activation transfer functions, while the Levenberg–Marquardt backpropagation algorithm (trainlm) is used as the training algorithm.

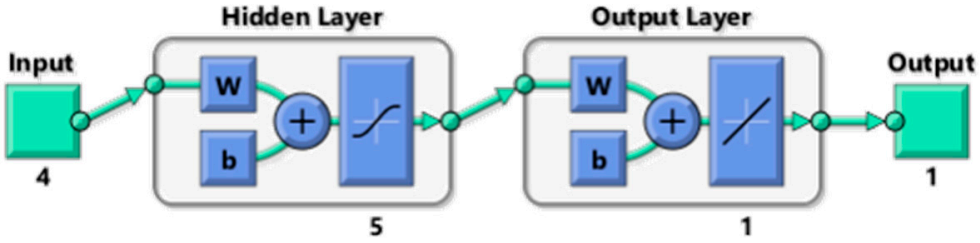

Figure 1. Architecture of the developed ANN.

3. Results and Discussion

3.1. Microhardness

The microhardness testing results (Figure 2) showed good repeatability of the results since the calculated standard deviations were below 7%. All nanocomposites showed more-or-less similar microhardness values, which was expected due to their similar microstructures [6,7]. Hardness typically increases with the increase in nanoparticle amount, but the interface between reinforcements and matrix as well as the distribution of reinforcements have a significant impact on composites hardness as well [13]. The uniform dispersion of the nanoparticles throughout the matrix is a demanding task, not easy to obtain [14]. The low influence of ceramic nanoparticles can be explained by the fact that their amount is very small and that the average Vickers microhardness indentation diagonal (approximately 85 μm) is significantly smaller than the distance between the nanoparticles, so the measured hardness values are most probably values of the nanocomposite matrix.

3.2. Wear Rate

The experiments were conducted according to the L24 orthogonal array, which is formed with Minitab 19 statistical package. The results of the wear tests for different combinations of factors are presented in Table 3. Wear rates were calculated for the whole testing period, i.e., they represented the total wear rates.

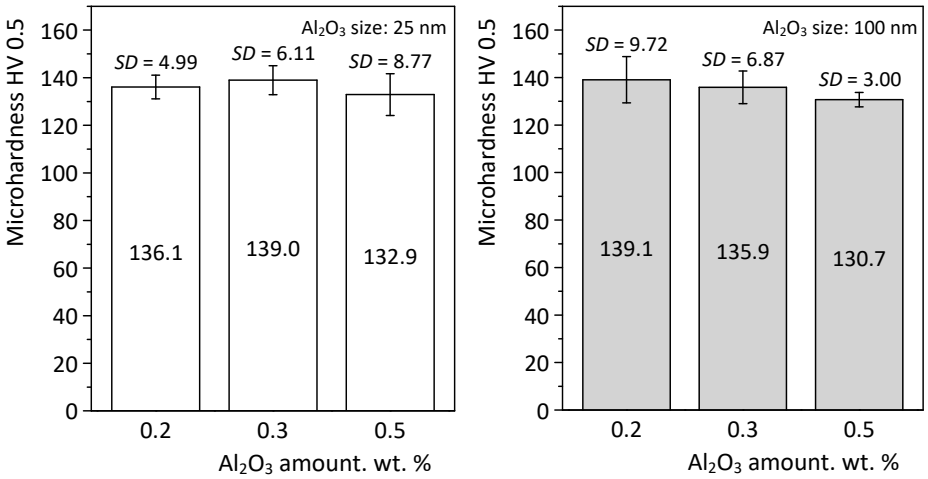

Figure 2. Microhardness values of tested nanocomposites with corresponding standard deviations (*SD*).

Table 3. Experimental design using L24 orthogonal array and obtained wear test results.

Test no.	Al_2O_3 Amount, wt. %	Al_2O_3 Size, nm	Sliding Speed, m/s	Normal Load, N	Wear Rate $\times 10^{-4}$, mm^3/m
1	0.2	25	0.25	40	1.671859
2	0.2	25	0.25	100	2.337679
3	0.2	25	1	40	0.701434
4	0.2	25	1	100	1.315875
5	0.2	100	0.25	40	0.940843
6	0.2	100	0.25	100	1.911662
7	0.2	100	1	40	0.150596
8	0.2	100	1	100	0.825748
9	0.3	25	0.25	40	0.851294
10	0.3	25	0.25	100	1.800392
11	0.3	25	1	40	0.630633
12	0.3	25	1	100	1.249261
13	0.3	100	0.25	40	0.573598
14	0.3	100	0.25	100	1.591235
15	0.3	100	1	40	0.055426
16	0.3	100	1	100	0.277412
17	0.5	25	0.25	40	0.414330
18	0.5	25	0.25	100	1.532718
19	0.5	25	1	40	0.141480
20	0.5	25	1	100	0.281368
21	0.5	100	0.25	40	0.200666
22	0.5	100	0.25	100	0.861667
23	0.5	100	1	40	0.013621
24	0.5	100	1	100	0.062987

Wear factors are also calculated in order to compare the obtained results with the literature data, using the well-known equation [15]. The obtained values were in the interval from 10^{-8} to 10^{-6} mm^3/Nm which corresponds to the literature data for metallic materials in sliding contact under boundary lubrication conditions [16]. This is in accordance with the used lubrication system, which delivers lubricant to the contact by the rotation of the disc. The disc is only partially sunk into the oil container and the contact between the block and the disc is above the oil level. This means that the contact is not fully supplied with the lubricant so mixed and boundary lubrication may occur.

Applying RSM to the experimental results, a second-order equation that determines the wear rate was created:

$$y = 2.015 - 6.3 \cdot A - 0.0077 \cdot B - 0.567 \cdot C + 0.0236 \cdot D + 4.4436 \cdot A^2 + 0.01112 \cdot A \cdot B + \\ + 1.316 \cdot A \cdot C - 0.0139 \cdot A \cdot D - 0.0012 \cdot B \cdot C - 0.000019 \cdot B \cdot D - 0.01135 \cdot C \cdot D \quad (1)$$

where: y is the wear rate and A, B, C and D are the Al_2O_3 amount, Al_2O_3 size, sliding speed and normal load, respectively.

The validity of the developed model was analysed using the analysis of variance (ANOVA) technique, for which results are shown in Table 4. The ANOVA was carried out for a significance level of 5%, i.e., for a confidence level of 95%. Sources with a p-value less than the significance level of 0.05 (5%) were considered to have a statistically significant contribution on the nanocomposite wear rate. This means that all considered influencing factors (Al_2O_3 amount, Al_2O_3 size, sliding speed and normal load) had a significant impact on wear rate. Regarding their interactions, only the interaction of sliding speed and normal load can be treated to have a significant impact on wear rate.

Table 4. Analysis of variance table for wear rate.

Source	Degree of Freedom	Adjusted Sums of Square	Adjusted Mean Square	F-Value	p-Value
Model	11	10.2340	0.93037	25.57	0.000
Linear	4	9.1493	2.28733	62.87	0.000
Al_2O_3 amount	1	2.5177	2.51766	69.20	0.000
Al_2O_3 size	1	1.1482	1.14815	31.56	0.000
Sliding speed	1	3.1590	3.15903	86.83	0.000
Normal load	1	2.3245	2.32447	63.89	0.000
Square	1	0.0406	0.04060	1.12	0.312
Al_2O_3 amount × Al_2O_3 amount	1	0.0406	0.04060	1.12	0.312
2-way interaction	6	0.6295	0.10491	2.88	0.056
Al_2O_3 amount × Al_2O_3 size	1	0.0649	0.06494	1.78	0.206
Al_2O_3 amount × sliding speed	1	0.0909	0.09094	2.50	0.140
Al_2O_3 amount × normal load	1	0.0649	0.06488	1.78	0.207
Al_2O_3 size × sliding speed	1	0.0069	0.00686	0.19	0.672
Al_2O_3 size × normal load	1	0.0109	0.01085	0.30	0.595
Sliding speed × normal load	1	0.3910	0.39099	10.75	0.007
Error	12	0.4366	0.03638		
Total	23	10.6706			

A normal probability plot of residuals (Figure 3) was used to verify the assumption that the residuals are normally distributed. As could be noticed, the prediction of wear rate with the formulated model is acceptable. The obtained R^2 (R-squared) value of 0.9591 and adjusted R^2 value of 0.9216 indicate a good fit of the model to the input data (R^2 = 1 is a perfect fit).

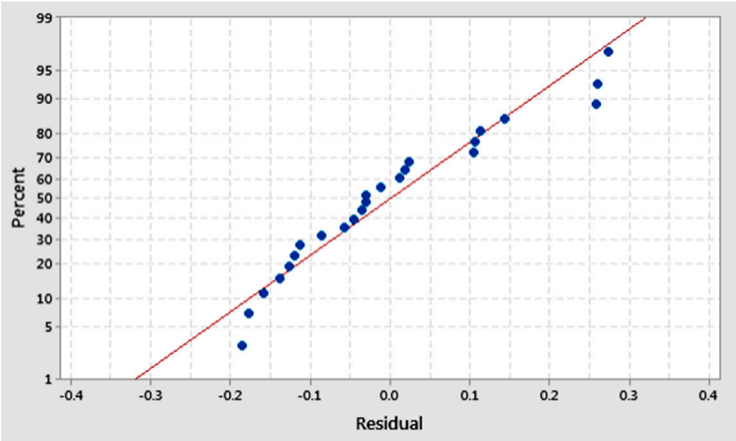

Figure 3. Normal probability plot for the developed RSM model.

The results of the wear rate prediction, obtained by using Equation (1) and presented in the form of wear maps, are shown in Figure 4. When creating the wear maps, two factors are set to the constant mean value (hold value), while the changes in the other two factors are shown on the diagram. Based on the presented wear maps, the lowest wear was

obtained for the nanocomposite with 0.5 wt. % Al_2O_3 of 100 nm size. The influences of the main influencing factors on wear rate are also presented as 3D wear curves in Figure 4g,h. Generally, all nanocomposites showed relatively low wear values. The average wear rates of the nanocomposites reinforced with smaller-size and bigger-size nanoparticles, at a sliding speed of 0.25 and a normal load of 100 N, are more than two times lower (approx. 56% and 66%, respectively) than the wear rate of thixocasted ZA-27 alloy [3], suggesting that the addition of nanoparticles can significantly improve wear resistance of the matrix. We obtained something similar in our previous research [17], where the addition of 1 wt. % Al_2O_3 nanoparticles (with particle size 20–30 nm) resulted in the reduction in the wear rate of modified ZA-27 alloy by approximately 60 %. Testing conditions and contact geometry were similar, i.e., the normal load was the same, but the sliding speed was higher (0.5 m/s) and lubricant viscosity (mineral engine oil SAE 15W-40, ACEA E3) was more than two times lower. Rohatgi and Schultz [1] in their review paper showed that for some MMnCs, addition of a small percentage of nanoparticles can affect specific material properties and that in some cases, the dispersed nanoparticles lead to property changes in the matrix itself.

As expected, testing under a higher normal load and lower sliding speed caused higher wear rates. This is according to the Stribeck curve in the area of mixed lubrication [18]. In that area, lubrication conditions become harsh with load increase and/or speed decrease. On the other hand, the increase in the Al_2O_3 particle size, as well as the Al_2O_3 particle amount, increased the wear resistance of nanocomposites. It was already shown in our previous study that the presence of nanoparticles led to the strengthening of the nanocomposites at room temperature and that the largest contribution was due to the enhanced dislocation density strengthening mechanism [6]. It was also shown that the strengthening effect was higher with the higher amount (wt. %) of nanoparticles. It is most probable that the contact temperature, together with contact pressure, induced other strengthening mechanisms (load transfer effect, Hall–Petch strengthening, Orowan strengthening, coefficient of thermal expansion and elastic modulus) that usually follow the addition of nanoparticles [2].

The microstructure and its influence on the mechanical characteristic of the tested nanocomposites were analysed in detail in our previous study [6]. The nanoparticles showed a tendency for agglomeration and formation of clusters due to the low wettability between them and the metal matrix. It was also shown that the microstructures were nondendritic and did not differ too much regardless of the size and amount of reinforcement. However, the nanocomposites reinforced with bigger Al_2O_3 nanoparticles had bigger grain sizes as well. The grain size was expressed through the average feret diameter which was 65 μm at nanocomposites reinforced with 0.3 wt. % of bigger-size nanoparticles and 55 μm at nanocomposites reinforced with 0.3 wt. % of smaller-size nanoparticles. This could be the reason why the increase in the Al_2O_3 particle size increased the wear resistance of nanocomposites. Bigger grains were harder to wear, which makes sense if we know that the widths of abrasive groves were from 10 to 20 μm (see wear mechanism discussion).

The experimental output values of the wear rates, shown in Table 2, are used for training, validation and testing of the ANN. It was trained using 70% of the data, while 15% was used for testing and 15% for validation. The performance of the modelled ANN is shown in Figure 5. Mean square error (MSE) for training initially has a high value which decreased to a very small value as the number of epochs increases, i.e., the ANN's training process is being performed correctly. Even though training continues until epoch 6, the best validation performance is achieved at epoch 0 with a value of 0.00031244, and the final value of the gradient coefficient at epoch 6 is very close to zero, i.e., 0.0014. The regression coefficient for training, validation and testing, as well as the overall regression coefficient of the network, was obtained and shown in Figure 6. The overall regression coefficient of the network was very close to 1 (R = 0.98729), indicating a good fit and good agreement between the experimental results and the ANN model prediction.

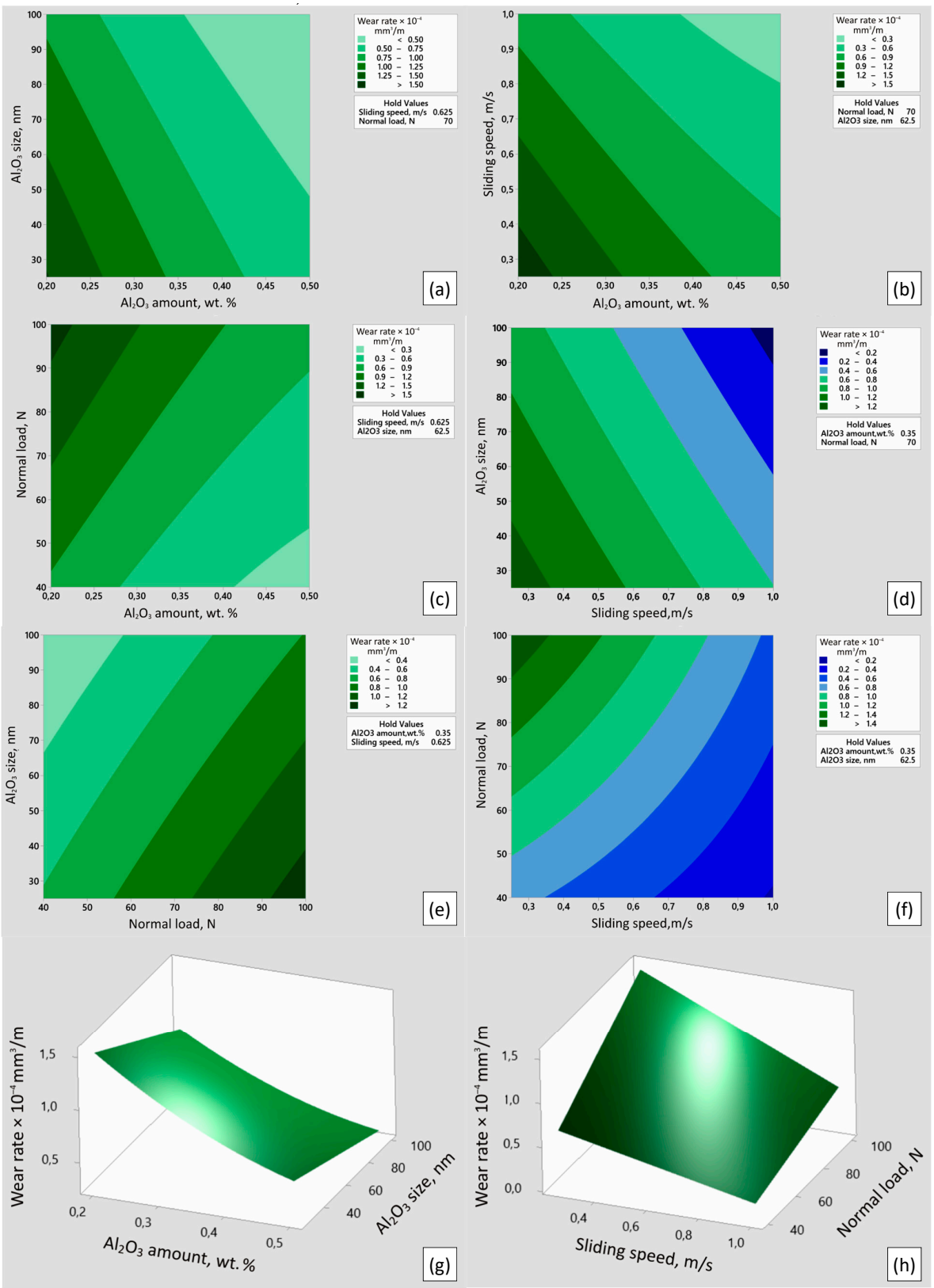

Figure 4. Wear maps for the tested nanocomposites, i.e., dependence of wear rate on: (**a**,**g**) Al_2O_3 amount and Al_2O_3 size, (**b**) Al_2O_3 amount and sliding speed and (**c**,**h**) Al_2O_3 amount and normal load, (**d**) Al_2O_3 size and sliding speed, (**e**) Al_2O_3 size and normal load and (**f**) sliding speed and normal load.

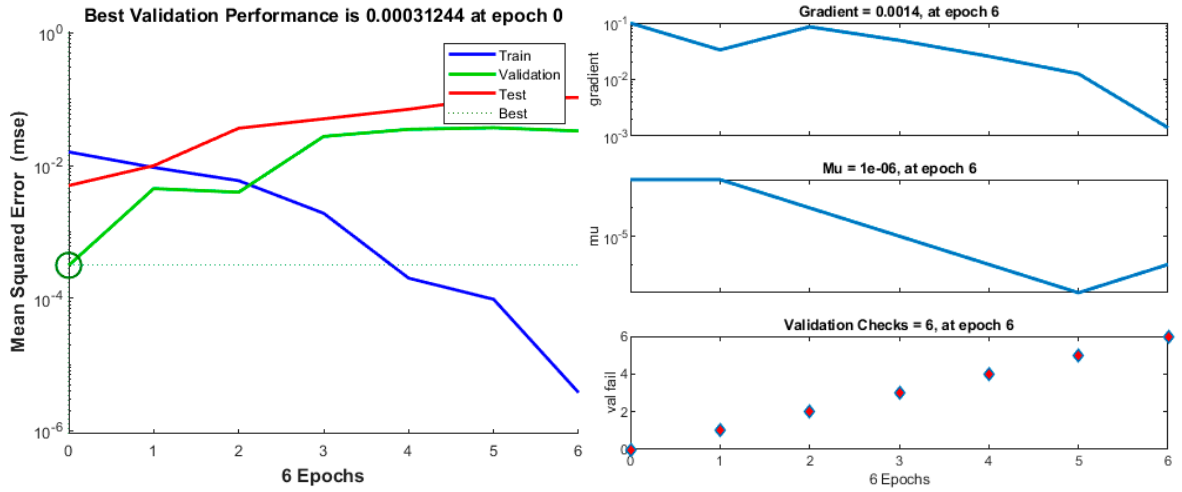

Figure 5. Performance of the modelled ANN—mean square error and training state plots.

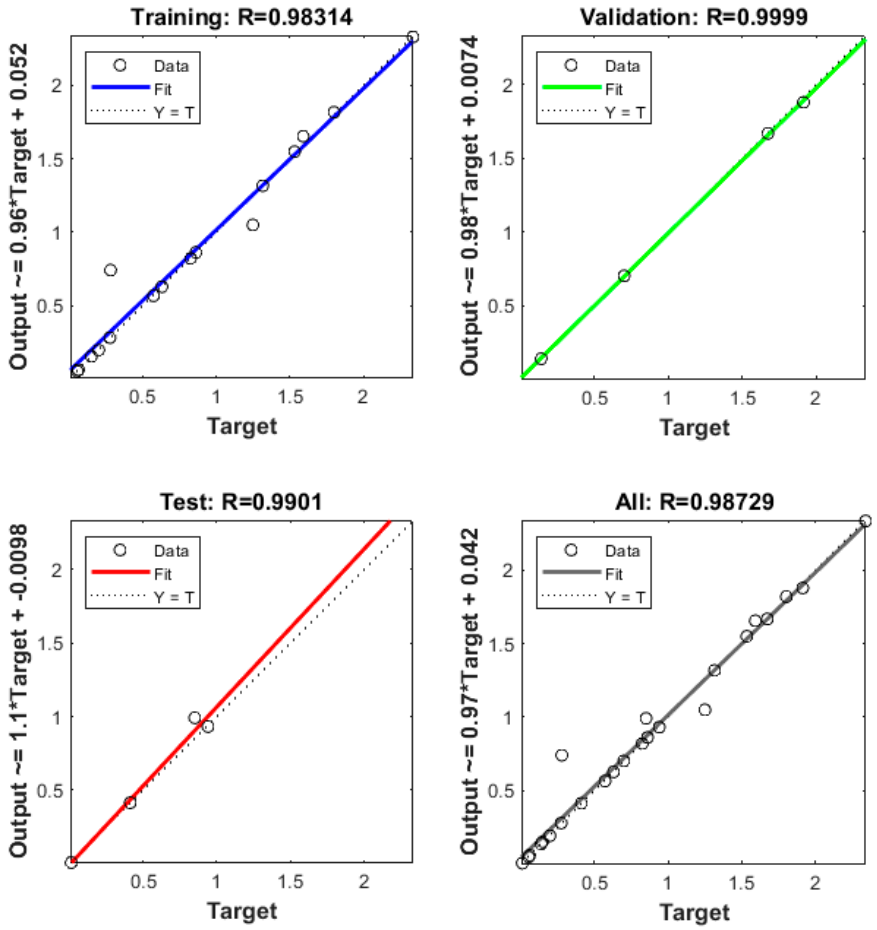

Figure 6. Accuracy of the modelled ANN—regression analysis of different phases.

The values of the wear rate predicted with the modelled RSM and ANN, within the limits of the experiment, are presented in Table 5 and compared with the experimental data. Its graphical interpretation is shown in Figure 7. In both cases (RSM and ANN prediction), there is a good correlation between experimental and predicted values and both prediction methods can be used with high reliability. However, values obtained by the modelled ANN are closer to experimental values; therefore, it can be concluded that in this case, the ANN is more efficient in predicting wear rate.

Table 5. Predicted values of the wear rate obtained by using the RSM and ANN.

Test no.	Wear Rate × 10^{-4}, mm^3/m			
	RSM Predicted	**RSM Error**	**ANN Predicted**	**ANN Error**
1	1.41255	0.259309	1.66686	0.004998
2	2.46300	−0.125321	2.33126	0.006419
3	0.82170	−0.120266	0.70289	−0.001455
4	1.36140	−0.045525	1.31694	−0.001060
5	0.92235	0.018493	0.93234	0.008505
6	1.88730	0.024362	1.87669	0.034968
7	0.26400	−0.113404	0.15359	−0.002993
8	0.71820	0.107548	0.82110	0.004648
9	1.00965	−0.158356	0.99211	−0.140817
10	1.97670	−0.176308	1.81776	−0.017371
11	0.51750	0.113133	0.62818	0.002449
12	0.97380	0.275461	1.04952	0.199744
13	0.60285	−0.029252	0.56660	0.006995
14	1.48440	0.106835	1.65411	−0.062870
15	0.04320	0.012226	0.05107	0.004356
16	0.41400	−0.136588	0.28120	−0.003788
17	0.47025	−0.055920	0.41495	−0.000617
18	1.27050	0.262218	1.54915	−0.016427
19	0.17550	−0.034020	0.14163	−0.000147
20	0.46500	−0.183632	0.74115	−0.459785
21	0.23025	−0.029584	0.19544	0.005228
22	0.94500	−0.083333	0.86240	−0.000736
23	−0.13200	0.145621	0.00828	0.005345
24	0.07200	−0.009013	0.06262	0.000362

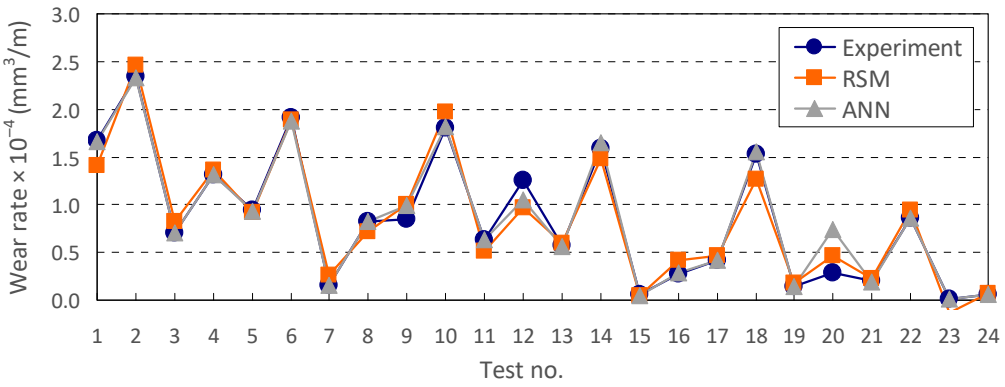

Figure 7. Comparison of experimental, RSM and ANN results.

3.3. Wear Mechanism

After testing, worn surfaces were examined using the SEM and EDS. The appearances of the worn surface did not differ too much regarding the test conditions. Worn surfaces of nanocomposites with different sizes of nanoparticles which had the highest wear were chosen as representative and shown in Figure 8. The dominant wear mechanism for all nanocomposites was abrasion, which is expected in mixed and boundary lubrication conditions. The presence of abrasive groves, with widths of approximately 10 to 20 μm, could be clearly noticed on all nanocomposites, but they are more pronounced and deeper on the nanocomposites reinforced with smaller-size nanoparticles. This is in accordance with the wear rate results, which showed that for the same testing conditions and the same amount of nanoparticles, nanocomposite reinforced with nanoparticles of approx. 25 nm (Figure 8a) showed a higher wear rate than the nanocomposite reinforced with nanoparticles of 100 nm (Figure 8b).

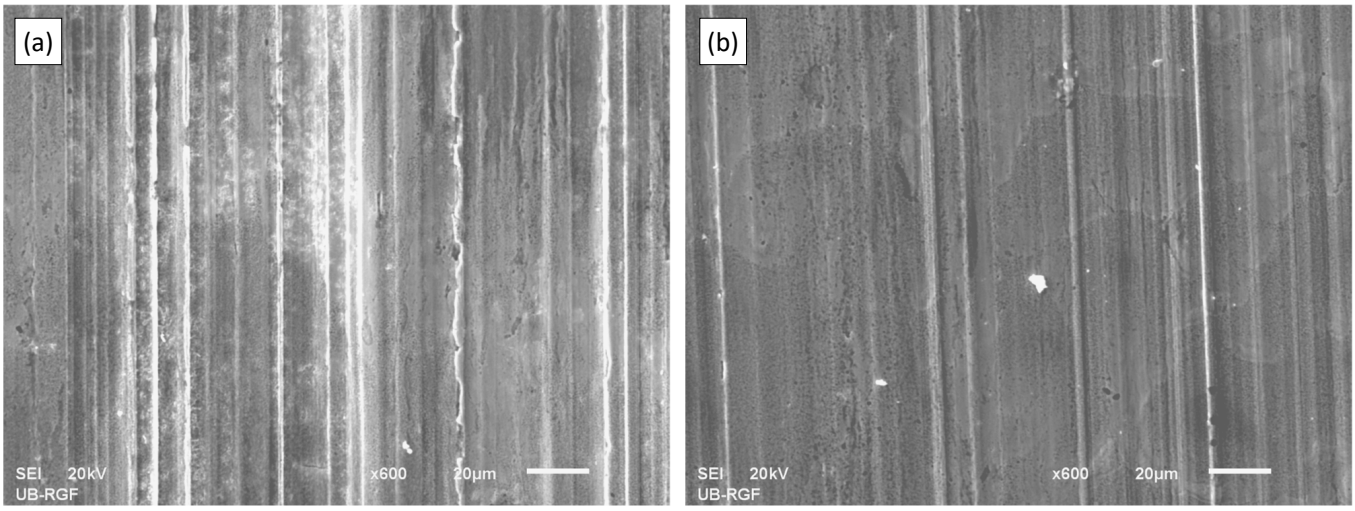

Figure 8. Worn surface of tested nanocomposites with 0.2 wt. % Al_2O_3 particles: (**a**) nanocomposite with particles approx. size of 25 nm and (**b**) nanocomposite with particles approx. size of 100 nm (testing conditions: 0.25 m/s; 1000 m; 100 N).

The EDS analysis results (Figure 9) of the worn surfaces presented in Figure 8 showed that there was no material transfer from the counter-body (steel disc) since the presence of Fe was not detected. The EDS analysis was performed in several points but only the most relevant results are presented in Figure 9. The presence of Al_2O_3 nanoparticles was not detected, since their size and amount were too small for this analysis. In some areas (Spectrum 4 and 18), higher amounts of Al were detected, but generally, the composition of the nanocomposites was according to the standard (Spectrum 1 and 21).

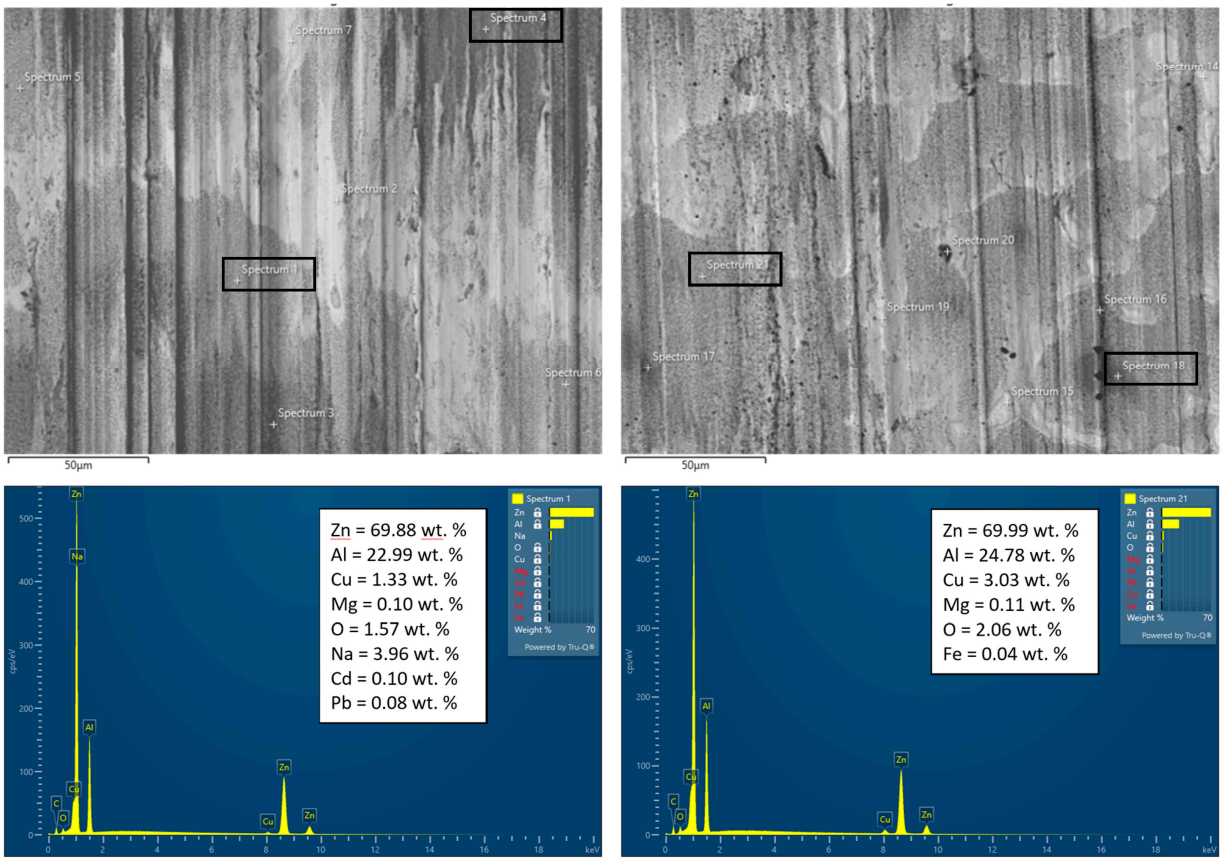

Figure 9. *Cont.*

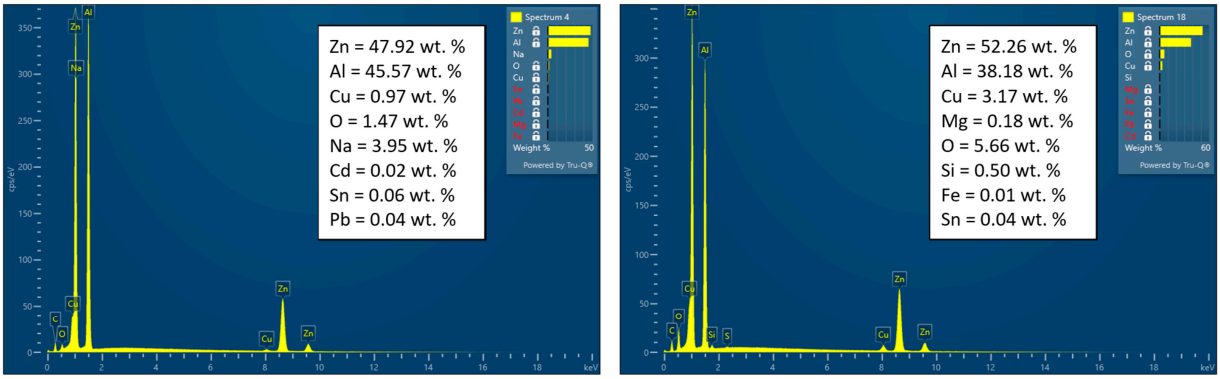

Figure 9. EDS analysis of worn surfaces shown in Figure 8.

4. Conclusions

The main aim of the research was to investigate the influence of the addition of a very small amount of Al_2O_3 nanoparticles, as well as the effect of the nanoparticles size on the wear resistance of the ZA-27 alloy. Wear characteristics were examined in lubricated sliding conditions. Tested nanocomposites were produced by a relatively cheap process which implied the infiltration of the previously treated nanoparticles (mechanical alloying of the matrix alloy scrap with nanoparticles) into the semi-solid matrix.

Analysis of variance (ANOVA) showed that all influencing factors (Al_2O_3 amount, Al_2O_3 size, sliding speed and normal load) had a significant impact on wear rate, while only the interaction of sliding speed and normal load can be treated to have a significant impact on wear rate. The increase in normal load and/or decrease in sliding speed increased the wear rate, while the increase in Al_2O_3 amount and Al_2O_3 size decreased the wear rate of the tested nanocomposites. Abrasion was the dominant wear mechanism for all nanocomposites, with abrasive grooves of approximate width from 10 to 20 μm. The abrasive groves were more pronounced and deeper on the nanocomposites reinforced with smaller-size nanoparticles, which is in accordance with the wear rate results. The presence of the transferred counter-body material was not noticed.

When compared to the experimental measurements, the results predicted by the RSM and ANN models were adequate. The obtained R^2 value for RSM was 0.9591 and the regression coefficient for ANN was $R = 0.99973$, i.e., both were very close to 1. However, the ANN was more efficient in the prediction of wear rate since their predicted values are closer to the experimentally measured values.

Author Contributions: Conceptualisation, A.V.; methodology, A.V. and B.S.; validation, S.K. and A.B.; formal analysis, A.V.; investigation, M.V.; writing—original draft preparation, A.V.; writing—review and editing, P.S. and M.H.; funding acquisition, A.V and B.S. All authors have read and agreed to the published version of the manuscript.

Funding: This work has been performed as a part of activities within the projects 451-03-68/2022-14/200105 and TR 35021, supported by the Republic of Serbia, Ministry of Education, Science and Technological Development, and its financial help is gratefully acknowledged. Petr Svoboda acknowledges the project FSI-S-20-6443, funded by the Ministry of Education, Youth and Sports of the Czech Republic. Simon Klančnik acknowledges the project BI-BA/21-23-036, funded by the Slovenian Research Agency. Marta Harničárová acknowledges the project VEGA 1/0236/21, funded by the Scientific Grant Agency of the Ministry of Education, Science, Research and Sport of the Slovak Republic. Collaboration through the CEEPUS network CIII-PL-0701 and bilateral Project 337-00-577/2021-09/16 between the Republic of Serbia and the Republic of Austria is also acknowledged.

Data Availability Statement: Not applicable.

Conflicts of Interest: The authors declare no conflict of interest.

References

1. Rohatgi, P.K.; Schultz, B. Lightweight metal matrix nanocomposites—Stretching the boundaries of metals. *Mater. Matters* **2007**, *2*, 16–20.
2. Casati, R.; Vedani, M. Metal matrix composites reinforced by nano-particles—A review. *Metals* **2014**, *4*, 65–83. [CrossRef]
3. Vencl, A.; Stojanović, B.; Gojković, R.; Klančnik, S.; Czifra, Á.; Jakimovska, K.; Harničárová, M. Enhancing of ZA-27 alloy wear characteristics by addition of small amount of SiC nanoparticles and its optimisation applying Taguchi method. *Tribol. Mater.* **2022**, *1*, 96–105. [CrossRef]
4. Shivakumar, N.; Vasu, V.; Narasaiah, N. Synthesis and characterization of nano-sized Al_2O_3 particle reinforced ZA-27 metal matrix composites. *Procedia Mater. Sci.* **2015**, *10*, 159–167. [CrossRef]
5. Çelebi, M.; Çanakçi, A.; Özkaya, S.; Karabacak, A.H. The effect of milling time on the mechanical properties of ZA27/Al_2O_3 nanocomposites. *Univers. J. Mater. Sci.* **2018**, *6*, 163–169. [CrossRef]
6. Bobić, B.; Vencl, A.; Ružić, J.; Bobić, I.; Damnjanović, Z. Microstructural and basic mechanical characteristics of ZA27 alloy-based nanocomposites synthesized by mechanical milling and compocasting. *J. Compos. Mater.* **2019**, *53*, 2033–2046. [CrossRef]
7. Vencl, A.; Bobić, I.; Bobić, B.; Jakimovska, K.; Svoboda, P.; Kandeva, M. Erosive wear properties of ZA-27 alloy-based nanocomposites: Influence of type, amount and size of nanoparticle reinforcements. *Friction* **2019**, *7*, 340–350. [CrossRef]
8. Vencl, A.; Bobić, I.; Jovanović, M.T.; Babić, M.; Mitrović, S. Microstructural and tribological properties of A356 Al-Si alloy reinforced with Al_2O_3 particles. *Tribol. Lett.* **2008**, *32*, 159–170. [CrossRef]
9. Stojanović, B.; Gajević, S.; Kostić, N.; Miladinović, S.; Vencl, A. Optimization of parameters that affect wear of A356/Al_2O_3 nanocomposites using RSM, ANN, GA and PSO methods. *Ind. Lubr. Tribol.* **2022**, *74*, 350–359. [CrossRef]
10. Vorkapić, M.; Mladenović, I.; Pergal, M.; Ivanov, T.; Baltić, M. Optimisation of tensile stress of poly(lactic acid) 3D printed materials using response surface methodology. *Tribol. Mater.* **2022**, *1*, 70–80. [CrossRef]
11. Yankov, E.; Minev, R.; Tonchev, N.; Lazov, L. Determination of the optimal mode of laser surface marking of aluminium composite panels with CO_2 laser. *Tribol. Mater.* **2022**, *1*, 114–119. [CrossRef]
12. Vencl, A.; Stojanović, B.; Miladinović, S.; Klobčar, D. Prediction of the wear characteristics of ZA-27/SiC nanocomposites using the artificial neural network. In Proceedings of the 6th International Scientific Conference "COMETa 2022", Jahorina, Bosnia and Herzegovina, 17–19 November 2022; pp. 107–114.
13. Rohatgi, P.K.; Liu, Y.; Ray, S. Friction and wear of metal-matrix composites. In *ASM Handbook, Friction, Lubrication, and Wear Technology*; Blau, P.J., Ed.; ASM International: Metals Park, OH, USA, 1992; Volume 18, pp. 801–811.
14. Karimzadeh, F.; Enayati, M.H.; Tavoosi, M. Synthesis and characterization of Zn/Al_2O_3 nanocomposite by mechanical alloying. *Mater. Sci. Eng. A* **2008**, *486*, 45–48. [CrossRef]
15. Vencl, A. Tribological behavior of ferrous-based APS coatings under dry sliding conditions. *J. Therm. Spray Technol.* **2015**, *24*, 671–682. [CrossRef]
16. Kato, K.; Adachi, K. Wear mechanisms. In *Modern Tribology Handbook*; Bhushan, B., Ed.; CRC Press: Boca Raton, FL, USA, 2001; Chapter 7.
17. Vencl, A.; Bobić, B.; Vučetić, F.; Svoboda, P.; Popović, V.; Bobić, I. Effect of Al_2O_3 nanoparticles and strontium addition on structural, mechanical and tribological properties of Zn25Al3Si alloy. *J. Braz. Soc. Mech. Sci. Eng.* **2018**, *40*, 513. [CrossRef]
18. Kandeva, M.; Kalitchin, Z.; Zadorozhnaya, E.; Vencl, A. Performance characteristics of lubricant based on rapeseed oil containing different amounts of metal-containing additive. *Ind. Lubr. Tribol.* **2022**, *74*, 309–315. [CrossRef]